

# Bosons and Fermions near Feshbach resonances

Henning Heiselberg §

Univ. of Southern Denmark, Campusvej 55, 5230 Odense M, Denmark

## Abstract.

Near Feshbach resonances,  $n|a|^3 \gg 1$ , systems of Bose and Fermi particles become strongly interacting/dense. In this unitary limit both bosons and fermions have very different properties than in a dilute gas, e.g., the energy per particle approach a value  $\hbar^2 n^{2/3}/m$  times an universal many-body constant. Calculations based upon an approximate Jastrow wave function can quantitatively describe recent measurements of trapped Bose and Fermi atoms near Feshbach resonances.

The pairing gap between attractive fermions also scales as  $\Delta \sim \hbar^2 n^{2/3}/m$  near Feshbach resonances and is a large fraction of the Fermi energy - promising for observing BCS superfluidity in traps. Pairing undergoes several transitions depending on interaction strength and the number of particles in the trap and can also be compared to pairing in nuclei.

## 1. Introduction

Recent experiments probe systems of bosons [1] and fermions [2, 3, 4, 5, 6] near Feshbach resonances by expansion and RF spectroscopy, where the interactions strengths and densities are large,  $n^{1/3}|a| \gg 1$ . In the Hamiltonian for a bulk system of  $N$  fermions or bosons

$$H = \sum_{i=1}^N \frac{\mathbf{p}_i^2}{2m} + \sum_{i<j} v(\mathbf{r}_i - \mathbf{r}_j), \quad (1)$$

interacting through two-body potentials  $v(r)$ , one can then no longer apply the dilute limit pseudo-potential approximation:  $v(r) = 4\pi\hbar^2 a \delta^3(\mathbf{r})/m$ , where  $a$  is the scattering length,

For example, the energy per particle in the dilute limit is

$$\frac{E}{N} = 2\pi\hbar^2 \frac{an}{m}, \quad n|a|^3 \ll 1, \quad (2)$$

for bosons and half that for the interaction energy of fermions in two spin states. It would lead to infinitely large positive and negative energies at Feshbach resonances,  $a \rightarrow \pm\infty$ . In stead the strongly or dense limit also known as the unitarity limit is encountered where energies (and pairing gaps) are predicted [7, 8] to approach

$$\frac{E}{N} = \text{constant} \times \hbar^2 \frac{n^{2/3}}{m}, \quad n|a|^3 \gg 1, \quad (3)$$

§ Danish Defense Research Establishment (hh@ddre.dk)

where the universal *constant* is a fundamental many-body parameter that only depends on the spin and the number of spin states of the particle. Several calculations and measurements of this constant now exist as will be discussed in detail below. On dimensional grounds the energy per particle is expected to scale with density as  $n^{2/3}$  independent of the scattering length  $|a| \rightarrow \infty$ . Thus both the Bose and Fermi interaction energies “fermionize” in the unitarity limit.

It is implicitly assumed that both the scattering length and the interparticle spacing  $r_0 = (3/4\pi n)^{1/3}$  are much larger than the range  $R$  of interaction which is usually the case for the cold atomic clouds. It is also the case for low density neutron matter since two neutrons are just unbound with  $^1S_0$  scattering length  $a = -18$  fm much larger numerically than the typical  $R \simeq 1$  fm range of nucleon-nucleon interactions. In contrast the neutron and proton are weakly bound as the deuterium atomic nucleus.

One of the predictions for the novel scaling laws in the unitarity limit for fermions [7] and bosons [8] were based on a calculation using the Jastrow ansatz for the two-body correlations also referred to as the lowest order constrained variation (LOCV) approximation [9]. This is a very useful model as it extends from both the dilute to the unitarity limit and analytically continues across Feshbach resonances  $a \rightarrow \pm\infty$ .

Studies of the transition from a Fermi gas of attractive atoms to a molecular BEC conventionally contain both atom and molecule components interacting resonantly (see, e.g., [10, 11, 12, 13, 14, 15]). The Jastrow approximation incorporates the strongly interacting limit including the transformation to molecules very differently. We shall argue that the transition from a Fermi gas to molecular BEC is smooth in the sense that two-body correlations gradually build up across the Feshbach resonance approaching the two-body wave function of molecules consisting of two bound Fermi atoms. The large size of the molecules near Feshbach resonances are therefore included in the two-body correlation function between atoms. The transition is continuous as  $a \rightarrow \pm\infty$  and will be described within LOCV.

We shall briefly outline the LOCV approximation and calculate the energy per particle in detail for both Bose and Fermi atoms in sections 2 and 3 respectively. We will show that the results compare well to recent data on Bosons [1] and Fermions [2, 3, 4] also near Feshbach resonances. In the remaining sections 4+5 we will discuss BCS pairing in atomic trap with attractive Fermions and draw a connection to pairing in nuclei and nuclear matter.

## 2. Bosons

The LOCV method was developed for strongly interacting correlated fluids as  $^4He$ ,  $^3He$  and nuclear matter in [9] and has more recently been applied to kaon condensation [16] and strongly interacting fermions [7] and bosons [8]. As explained in these references the Jastrow wave function

$$\Psi_J(\mathbf{r}_1, \dots, \mathbf{r}_N) = \prod_{i < j} f(\mathbf{r}_i - \mathbf{r}_j), \quad (4)$$

incorporates essential two-body correlations and is a good approximation for cold dilute and dense bose systems. We shall extend this wave function to fermions in the next section. The pair correlation function  $f(r)$  can be determined variationally by minimizing the expectation value of the energy,  $E/N = \langle \Psi | H | \Psi \rangle / \langle \Psi | \Psi \rangle$ , which may be calculated by Monte Carlo methods that are fairly well approximated by including only two-body clusters. The basic idea of this method (LOCV) is that for  $r < r_0$  the Jastrow function  $f(r)$  approximately obeys the Schrödinger equation for a pair of particles

$$\left[ -\frac{\hbar^2}{m} \frac{d^2}{dr^2} + v(r) \right] r f(r) = \lambda r f(r), \quad (5)$$

where the eigenvalue energy of two atoms  $\lambda = 2E/N$ . To take into account many-body effects, which become important when  $r$  is comparable to  $r_0$ , the conditions  $f(r > d) = 1$  and  $f'(r = d) = 0$  are imposed at the healing distance  $d$ , which is determined self consistently from number conservation

$$n \int_0^d f^2(r) d^3r = 1. \quad (6)$$

In the dilute limit  $f(r) \simeq 1$  and so  $d = r_0$  whereas in the dense limit  $d = (2/3)^{1/3} r_0$ . Generally  $d \simeq r_0$ .

When the range  $R$  of the two-body potential  $v(r)$  is small compared to both  $|a|$  and  $r_0$ , the boundary condition at short distances is given by the scattering length  $(rf)'/rf = -1/a$  at  $r = 0$ . Solving the Schrödinger equation gives a wave-function  $rf(r) \propto \sin[k(r - b)]$  for positive energies. The boundary conditions and normalization determine the phase  $kb$ , the energy and the healing length  $d$ . When positive, the energy  $E/N = \hbar^2 k^2 / 2m$  is calculated in terms of the scattering length (see [8] for details)

$$\frac{a}{d} = \frac{\kappa^{-1} \tan \kappa - 1}{1 + \kappa \tan \kappa}, \quad (7)$$

where  $\kappa = kd$ .

There is also a negative energy solution as shown in Fig. 1. For negative scattering lengths such many-boson systems are unstable towards collapse whereas the many-fermion system is stable as will be discussed below. Furthermore, the negative energy solution for both bosons and fermions, when the scattering length cross over from large and negative to positive, corresponds to the molecular BEC as we shall see shortly. The solution for wave function to the Schrödinger Eq. (5) is  $rf(r) \propto \sinh[k(r - b)]$  or  $rf(r) \propto \cosh[k(r - b)]$ . The energy  $E/N = -\hbar^2 k^2 / 2m$  is determined by

$$\frac{a}{d} = \frac{\kappa^{-1} \tanh \kappa - 1}{1 - \kappa \tanh \kappa}. \quad (8)$$

The multiple solutions to Eqs. (8) and (7) corresponding to 0,1,2,3... number of nodes in the (two-body) wave-function  $f(r)$  are shown in Fig. (1). In the limit  $R \rightarrow 0$  nodes inside the two-body potential and deeply bound states are irrelevant.

In the dilute limit  $|a| \ll r_0$  Eqs. (7) and (8) give the correct energy per particle, Eq. (2). By contrast, in the unitarity limit  $|a| \gg r_0$ , Eq. (7) reduces to  $\kappa \tan \kappa = -1$  with solutions  $\kappa_1 = 2.798386..$ ,  $\kappa_2 = 6.1212..$ , etc., and asymptotically  $\kappa_n = n\pi$  for integer  $n$ .

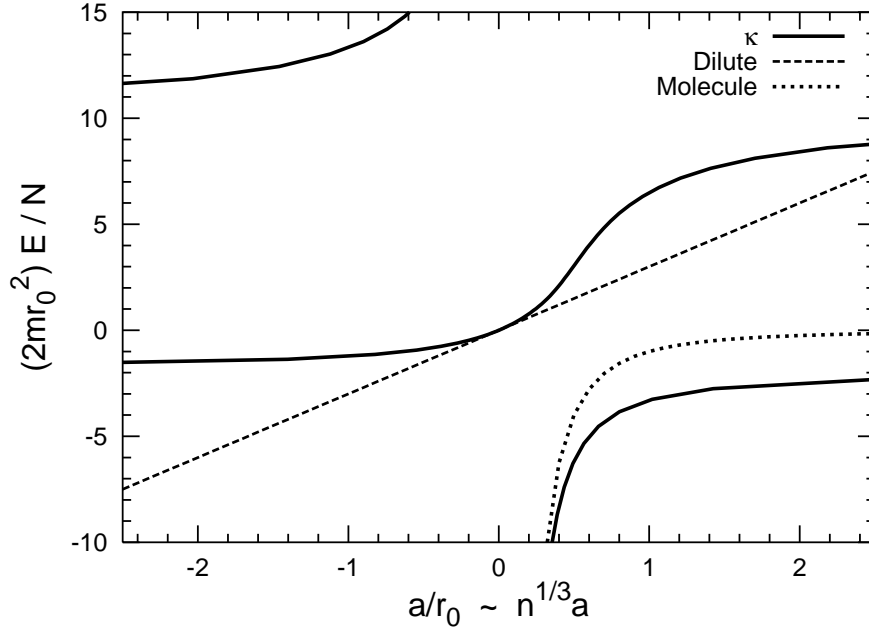


**Figure 1.** LOCV calculation of the energy per particle  $(2mr_0^2)E/N \simeq \pm\kappa^2$  in a BEC vs. scattering length. Dashed line is the dilute limit result whereas the dotted line is half the molecule energy in vacuum  $E/N = -\hbar^2/2ma^2$ .

The negative energy solution to Eq. (8) reduces in the unitarity limit to  $\kappa \tanh \kappa = 1$  for  $a \gg r_0$  with solution  $\kappa_0 = 1.1997\dots$ . As the scattering length cross over from  $-\infty$  to  $+\infty$  the negative energy state is analytically continued towards the molecular bound state with  $E/N = -\hbar^2/2ma^2$  as  $a \rightarrow +0$ . Therefore the LOCV approximation to many-body systems correctly reproduces the energies in both the dilute limit and the molecular limit. In the unitarity limit it correctly predicts qualitatively the  $n^{2/3}$  scaling of particle energies of Eq. (3). Quantitative comparison to experimental data for cold bose and fermi atoms in the unitarity limits will be given below.

The energy of a repulsive BEC gas as it approaches a Feshbach resonance,  $a \rightarrow +\infty$ , is of special interest

$$\frac{E_1}{N} = \left(\frac{3}{2}\right)^{2/3} \frac{\hbar^2 \kappa_1^2}{2mr_0^2} = 13.33 \hbar^2 \frac{n^{2/3}}{m}. \quad (9)$$

These energies can be compared to the JILA experiment [1] where the scattering length is tuned near the Feshbach resonance by a magnetic field  $B$  as

$$a(B) = a_{bg} \left(1 - \frac{\Delta}{B - B_{Feshbach}}\right). \quad (10)$$

Coherent atom-molecule oscillations are induced in the BEC at a frequency  $\nu(B)$ . We take this frequency as the difference between the mean field energy of two atoms in the atomic state and the molecular state

$$\nu = \frac{2}{h} \frac{E_+ - E_-}{N} = \frac{\hbar}{2\pi m d^2} (\kappa_+^2 - \kappa_-^2). \quad (11)$$

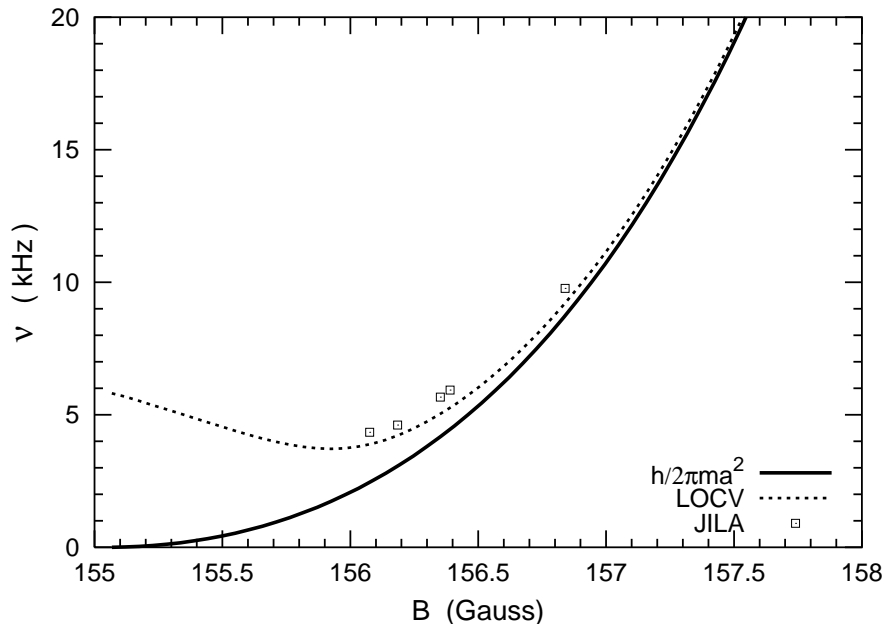


**Figure 2.** Frequency of the atomic-molecular transition in a  $^{85}\text{Rb}$  BEC as function of magnetic field near the Feshbach resonance. The full curve is the in vacuum transition frequency for two atoms to a molecule  $\nu = \hbar/2\pi ma^2$ . The LOCV prediction of Eq. (11) for the transition of two atoms to a molecule in the many-body system is shown with dashed curve. Data from JILA [1].

Here, the indices + and - refer to the (lowest) positive and negative energy branches of Fig. (1) respectively as function of  $a$ . The negative energy branch approaches the molecular energy, i.e.  $E_-/N \simeq -\hbar^2/2ma^2$  as  $a \rightarrow +0$ . The resulting frequency is shown in Fig. (2).

At the Feshbach resonance the LOCV frequencies approaches a constant value which according to Eqs. (11) is  $\nu = \hbar(\kappa_1^2 + \kappa_0^2)/2\pi md^2 = 2.51\hbar n^{2/3}/m$  for the transition of two atoms in the unitarity limit to a molecular state. For the  $^{85}\text{Rb}$  BEC of average density  $n = 2 \times 10^{-12}\text{cm}^{-3}$  [1] this results in a frequency  $\nu = 5.9\text{kHz}$  at the Feshbach resonance as seen in Fig. (2). The calculated transition frequency is in nice agreement with the JILA data close to the resonance. The calculated frequencies have a minimum just above the resonance of order  $\sim 4\text{kHz}$  because the atomic energy decrease faster with detuning (i.e., decreasing scattering length) than the molecular energy.

The absence of experimental data in the 155-156G region is due to overdamping of the atom-molecule oscillations. The imaginary part of the self-energies may in this region be so large near the Feshbach resonance that the quasi-particles are not well defined.

The effective range has been neglected in our calculations because we have assumed that the range of interaction is small as compared to scattering lengths and interparticle distances. The effective range of the interaction is by definition equal to the range for a square well potential. However, when the two-body interaction has a long tail and the

scattering length is not large, then corrections to the scattering amplitude and particle energies from the effective range appear. This is the case in Fig. (2) off the resonance where the scattering length becomes small. Around  $B \gtrsim 157\text{G}$  the frequency is slightly increased [17] improving the agreement with data.

The depletion of the condensate can also be calculated in the LOCV approximation from  $f(r)$ . The condensate fraction is [8]

$$\frac{n_0}{n} = 1 - n \int [1 - f(r)]^2 d^3r = \left(\frac{d}{r_0}\right)^3 \left[ \frac{6}{\kappa^3} (\sin \kappa - \kappa \cos \kappa) - 1 \right], \quad (12)$$

which predicts quenching of the BEC for  $na^3 \gtrsim 0.6$ . The condensate fraction differs from the dilute limit fraction:  $n_0/n = 1 - (4/\sqrt{3}\pi)(a/r_0)^{3/2}$ , as well as from the hard-sphere potential and exact quantum Monte Carlo calculations.

The three-boson problem cannot generally be described by the scattering length only but depends on a three-body parameter as well [18] which is referred to as non-universality. It was shown in [19], however, that for three bosons in a trap the energy was universal in both the dilute and in the unitarity limit - but not between these limits. Thus we may expect that the many-boson problem is universal as well in these two limits. The three-fermion problem is simpler in the sense that the Pauli exclusion principle prohibits Efimov states and therefore no three-body parameter enters, and the three- and many-body problem is universal.

### 3. Fermions

In the unitarity limit,  $n|a|^3 \gg 1$ , a system of fermions is dense and/or strongly interacting. The energy per particle has been calculated within Galitskii resummation, the LOCV method and recently by fixed node Green's function Monte Carlo (FN-GFMC). They find that the interaction energy does not extrapolate to  $\pm\infty$  as the dilute result of Eq. (2) does, but approaches a universal constant times the kinetic or Fermi energy,  $E_F = \hbar^2 k_F^2 / 2m$ , as in Eq. (3)

$$\frac{E}{N} = E_{kin} + E_{int} = \frac{3}{5} E_F [1 + \beta]. \quad (13)$$

Here,  $\beta = E_{int}/E_{kin}$  is a universal many-body parameter in the unitarity limit, which only depends on the number of spin states  $s$  through the Pauli principle and the density  $n = s k_F^3 / 6\pi$ . For two spin states  $\beta$  is displayed in Table 1 for the various calculations and recent experiments as will be described in the following subsections. Recent measurements [2, 3, 4, 5, 6] of  $\beta$  seem to confirm this unitarity limit near Feshbach resonances.

#### 3.1. Galitskii resummation

The scattering amplitude, which in the dilute limit is simply  $f = -a$ , can in the interacting many-body system be expanded in powers of scattering length via Galitskii resummation of ladder diagrams [20]. It was shown in [7] that resummation of scattering

**Table 1.** Calculations and measurements of the ratio of interaction to kinetic energy  $\beta = E_{int}/E_{kin}$  in the dense/strongly interacting regime  $a \rightarrow -\infty$  for two spin states.

$-\beta$	Calc./Exp.	Reference
$0.26 \pm 0.07$	Duke exp.	[2]
0.3-0.4	ENS exp.	[3]
0.4-0.6	JILA exp.	[4]
$0.68 \pm 0.1$	Innsbruck exp.	[6]
0.67	Galitskii approx.	[7]
0.54	LOCV approx.	[7]
$0.56 \pm 0.01$	FN-GFMC	[25]

amplitudes lead to a  $f \sim k_F^{-1}$  scaling of the real part of the scattering amplitude in the unitarity limit. Brueckner, Bethe and Goldstone [21] pioneered such studies for nuclear matter and  ${}^3\text{He}$ , which are more complicated cases since the range of interactions, scattering lengths and repulsive cores all are comparable in magnitude. In our case the range  $R$  of interaction is small,  $k_F R \ll 1$ , and therefore all particle-hole diagrams are negligible. This is opposite to electro-magnetic interactions where the strength of the interaction is small but the range of interactions is large and must be screened by Debye or Landau damping implicit in loop diagrams. In the Galitskii resummation all higher order particle-particle and hole-hole diagrams are found to contribute to the same order when  $k_F |a| \gg 1$ . Due to the very restricted phase space such higher order terms are usually neglected as in standard Brueckner theory. Truncating the resummation to second order one finds for two spin states [7] that  $\beta = -175/27(11 - 2 \ln 2) = -0.67$  in the unitarity limit.

### 3.2. LOCV

The unitarity limit can also be studied in the LOCV approximation. For fermions the many-body wave function must be anti-symmetric. To first approximation one includes a Slater wave function ( $\Phi$ ), which is the ground state of free fermions

$$\Psi_{JS}(\mathbf{r}_1, \dots, \mathbf{r}_N) = \Phi \prod_{i < j'} f(\mathbf{r}_i - \mathbf{r}_{j'}), \quad (14)$$

We refer to Ref. [25] where also a BCS wave function including pairing is employed. Because  $\Phi$  insures that same spins are spatially anti-symmetric, the Jastrow wave function only applies to particles with different spins (indicated by the primes). Therefore, the number conservation also applies to different spin states only and Eq. (6) should be multiplied by a factor  $(s-1)/s$  on the left hand side which affects the healing length. For example, in the unitarity limit  $a \rightarrow -\infty$  the healing length now approaches  $d = r_0(2s/(s-1)3)^{1/3} = (3\pi/(s-1))^{1/3}k_F^{-1}$ .

Otherwise the LOCV calculation for fermions follows the lines as for bosons and the interaction energy is  $E_{int} = \kappa^2/2md^2$  as calculated above. In addition the kinetic energy  $(3/5)E_F$  appears due to the Slater ground state. The total energy becomes

$$\frac{E}{N} = \frac{3}{5}E_F \pm \frac{\hbar^2\kappa^2}{2md^2}, \quad (15)$$

where the  $\pm$  refers to the positive and negative energy states discussed above. The energy becomes [22]

$$\frac{E}{N} = \frac{3}{5}E_F - \frac{\hbar^2\kappa_0^2}{2md^2} = E_F \left[ \frac{3}{5} - \left( \frac{s-1}{3\pi} \right)^{2/3} \kappa_0^2 \right]. \quad (16)$$

With  $\kappa_0 = 1.1997..$  we thus obtain in the unitarity limit  $\beta = 0, -0.54, -0.85, -1.12, \dots$ , for  $s = 1, 2, 3, 4, \dots$  respectively.

For the gas to be stable towards collapse the energy must be positive, i.e.,  $1 + \beta > 0$ . Therefore the LOCV approximation predicts that up to  $s \leq 3$  spin states are stable in the unitarity limit whereas in the Galitskii approximation only  $s = 1, 2$  are stable. The marginal case  $s = 3$  may be studied with  ${}^6\text{Li}$  atoms since they have three spin states with broad and close lying Feshbach resonances [5]. The stability of two spin states towards collapse has recently been confirmed for a  ${}^6\text{Li}$  and  ${}^{40}\text{K}$  gases near Feshbach resonances. It has long been known that neutron star matter [23] with two spin states likewise has positive energy at all densities whereas for symmetric nuclear matter with two spin and two isospin states, i.e.  $s = 4$ , the energy per particle is negative. Nuclear matter is therefore unstable towards collapse and subsequent implosion, spinodal decomposition and fragmentation at subnuclear densities[24]. Above nuclear saturation densities,  $k_F R \gtrsim 1$ , short range repulsion stabilizes matter up to maximum masses of neutron stars  $\sim 2.2M_\odot$ , where gravitation makes such stars unstable towards collapse.

### 3.3. Fixed-node Green's function Monte Carlo (FN-GFMC)

In Ref. [25] the energy of a finite number of Fermions in a box has been calculated within FN-GFMC at a Feshbach resonance. Since the gas is in a meta-stable state with typical  $\sim 40$  lower lying molecular states, the number of nodes in the Jastrow two-body wave-function must be fixed in Monte Carlo calculations. At the Feshbach resonance  $a \rightarrow -\infty$  they find that the energy of the system increase with the number of particles as  $E = (1 + \beta)NE_{kin}$  with  $\beta = -0.56 \pm 0.01$ . This is an upper limit since FN-GFMC is also a variational calculation of the energy.

Pairing favors an even number of particles and from the odd-even staggering of  $E(N)$  a pairing gap  $\Delta \simeq 0.54E_F$  is extracted from the FN-GFMC calculations at the Feshbach resonance.

When comparing the various calculations of  $\beta$  it should be noted that the FN-GFMC value  $\beta = -0.56$  includes pairing energies whereas the LOCV and the Galitskii approximations did not. Excluding pairing the FN-GFMC leads to a higher energy state with  $\beta = -0.44$  [25]. In comparison the expected contribution  $(3/8)\Delta^2/E_F$  from



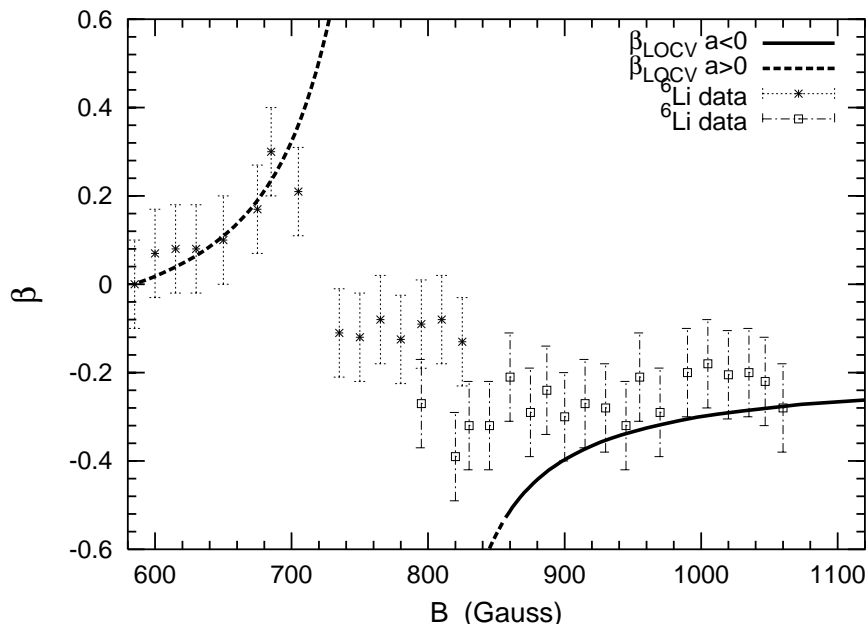


**Figure 3.** Ratio  $\beta$  of the interaction energy over the kinetic energy vs. magnetic field for  ${}^6\text{Li}$ . Predictions from Eq. (15) with  $\kappa$  calculated within LOCV are shown with full and dashed curves for negative and positive scattering length respectively. The data, density and scattering length vs. magnetic field near the Feshbach resonance at 855G is taken from [3].

pairing energies in the dilute limit would lead to an even larger correction if the pairing gap in the unitarity limit is inserted.

### 3.4. Experiments

Several experiments with trapped Fermi atoms have recently measured energies in the strongly interacting or dense limit near Feshbach resonances. The energy in the trap (excluding that from the harmonic oscillator potential) is  $E/N = (3/8)E_F\sqrt{1+\beta}$  where  $E_F = (3N)^{1/3}\hbar\omega$  is the Fermi energy in a trapped non-interacting gas.

The Duke group [2] measured the energy of  ${}^6\text{Li}$  Fermi atoms near a Feshbach resonance from expansion energies. After correcting for thermal energies, they find  $\beta = -0.26 \pm 0.01$  close to the Feshbach resonance  $k_F a \simeq -7.4$ .

Bourdell et al. at ENS [3] measure expansion energies for  ${}^6\text{Li}$  near a Feshbach resonance. They find  $\beta = -0.4 \pm 0.1$  as  $a \rightarrow -\infty$  as shown in Fig. (3). The situation is more complicated at the other side of the resonance for positive  $a$ , where the ratio increases up to  $\beta = 0.2 \pm 0.1$  in agreement with LOCV predictions, but then drops to a plateau close to the resonance. The LOCV calculations compare well to ENS data as  $a \rightarrow -\infty$  whereas  $\beta(a \rightarrow +\infty)$  exceeds the data especially at the plateau. Whether this is due to molecule formation [26] or finite temperature, which can have a strong effect on  $\beta$  [27], should be investigated.

The MIT experiment [5] on  ${}^6\text{Li}$  and the JILA experiment on  ${}^{40}\text{K}$  [4] measure the transition frequency between three hyperfine states which confirm the unitarity limitation to energies and frequencies. The JILA experiment is performed at two densities and does not find a plateau. In extracting the JILA value for  $\beta$  as given in Table 1, the reduction factor  $(s - 1)$  in Eq. (16) is replaced by  $s$  because of the specific population of spin states in their RF experiment.

With the discovery of a molecular BEC the Innsbruck group [6] has been able to measure the size of the atomic cloud, which scales with  $(1 + \beta)^{1/4}$ , around the Feshbach resonance at very low temperatures. They find  $\beta = -0.68 \pm 0.1$  compatible with the theoretical estimates.

#### 4. Pairing of Fermi atoms in harmonic oscillator traps

BCS pairing and superfluidity is expected for trapped Fermi atoms with attractive interactions. As atomic gases have widely tunable number of particles, densities, interaction strengths, temperatures, spin states, and other parameters, they hold great promise for a more general understanding of pairing phenomena in solids, metallic clusters, grains, nuclei, neutron stars and quark matter.

In a uniform dilute gas with sufficiently strong interactions or large number of particles the bulk limit is reached, and the pairing gap is at zero temperature [28, 29]

$$\Delta = E_F \frac{8}{e^2} (4e)^{s/3-1} \exp \left[ \frac{\pi}{2ak_F} \right]. \quad (17)$$

In the unitarity limit,  $k_F|a| \gtrsim 1$ , the pairing gap approaches a finite fraction of the Fermi energy [7] just as the energy per particle. The FN-GFMC calculations discussed above [25] find that the odd-even staggering energy or pairing gap in bulk is  $\Delta \simeq 0.54E_F$  which is quite close the value  $\Delta \simeq 0.49E_F$  obtained by extrapolating Eq. (17) to  $a \rightarrow -\infty$  for two spin states.

Near a Feshbach resonance the strongly interacting Fermi gas becomes unstable towards molecule formation and the critical temperature  $T_c = (\gamma/\pi)\Delta \simeq 0.567\Delta$  for BCS superfluidity is expected to cross-over towards the slightly smaller critical temperature for forming a Bose-Einstein condensate of molecules [30, 31]. If we take  $\Delta = 0.54E_F$  from FN-GFMC both the BCS and BEC critical temperatures,  $T_c \simeq 0.5\Delta$ , are therefore around or above the lowest temperatures reported for trapped Fermi atoms [2, 3, 4, 5, 6]. This bodes well for observing BCS superfluidity in atomic traps and establishing the unitarity scaling of pairing gaps.

As cooling improves further and smaller pairing gaps may be found, new pairing regimes take over that are important in other systems as solids, nuclei, neutron stars, etc. We shall outline the various pairing regimes shown in Fig. (4) vs. density interaction strength and relate it to BCS pairing in bulk.

The various pairing regimes shown in Fig. (4) can, except from the dense or

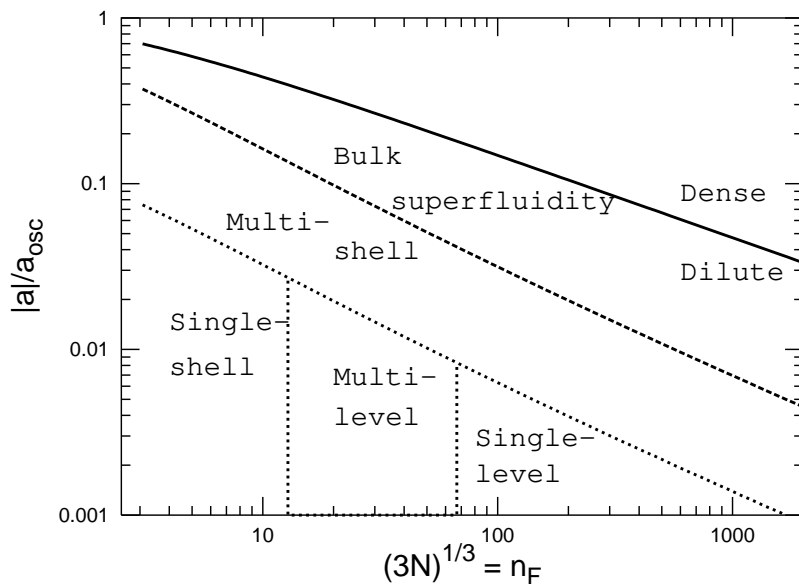


**Figure 4.** Diagram displaying the regimes for the various pairing mechanisms (see text) at zero temperature in h.o. traps vs. the number of particles  $N = n_F^3/3$  and the interaction strength  $a < 0$ . The dotted lines indicate the transitions between single-shell pairing  $\Delta = G$ , multi-level, single-level, and multi-shell pairing. At the dashed line determined by  $2G \ln(\gamma n_F) = \hbar\omega$  the pairing gap is  $\Delta \simeq \hbar\omega$ , and it marks the transition from multi-shell pairing to bulk superfluidity Eq. (17). The pairing gap is  $\Delta = 0.54E_F$  above the full line  $n|a|^3 \geq 1$ , which separates the dilute from the dense gas. From [32]

unitarity limit, be calculated from in the dilute limit Hamiltonian

$$H = \sum_{i=1}^N \left( \frac{\mathbf{p}_i^2}{2m} + \frac{1}{2} m \omega^2 \mathbf{r}_i^2 \right) + 4\pi \hbar^2 \frac{a}{m} \sum_{i < j} \delta^3(\mathbf{r}_i - \mathbf{r}_j), \quad (18)$$

for  $N$  atoms in a spherical harmonic oscillator (h.o.) potential. When energies are measured in units of  $\hbar\omega$ , and lengths in  $a_{osc} = \sqrt{\hbar/m\omega}$  only two parameters remain in the Hamiltonian, namely the number of particles and the interaction strength as plotted in Fig. (4)

When the traps contain relatively few atoms that are weakly interacting (lower left corner of Fig. (4)) the level spectra are highly degenerate due to the SU(3) symmetry of the spherical h.o. potential. Due to the Pauli principle the h.o. shells  $n = 0, 1, \dots, n_F$  are filled up. Only the top Fermi shell  $n_F \simeq (3N)^{1/3}$ , where  $N$  is the number of Fermi atoms, may be partially filled. The levels with angular momentum  $l = n_F, n_F - 2, \dots, 1$  or  $0$  are all degenerate in the weakly interacting limit due to SU(3) symmetry. Consequently, pairing is enhanced as the gap generally increases with the number of states, and leads to a supergap [33]

$$G = \frac{32\sqrt{2n_F}}{15\pi^2} \frac{|a|}{a_{osc}} \hbar\omega. \quad (19)$$

For stronger interactions multi-shell pairing also takes place whereas for more particles

the stronger mean field cause level splitting, which reduce pairing towards single level pairing [33, 34, 32] and shows up as a distinct shell structure with h.o. magic numbers.

Varying the number of particles and interaction strengths thus allows us to investigate a wide range of pairing mechanisms that apply to many other physical systems, e.g., nuclei and neutron stars as will be discussed in the following section.

## 5. Pairing in nuclei and nuclear matter

The nuclear mean field is often approximated by a simple h.o. form and the residual effective pairing interaction by a delta force in order to obtain some qualitative insight into single particle levels, pairing, collective motion, etc., (see, e.g., [35, 36]). We can therefore compare pairing in nuclei to that in traps as investigated above, once the h.o. potential is adjusted to describe nuclei.

As described in [32] the anharmonic nuclear mean field is stronger and of opposite sign than that in atomic traps. It also contains a strong spin-orbit force which change the magic numbers from the h.o. shells. Correcting for that the quasi-particle energies and pairing gaps were calculated by solving the Bogoliubov-deGennes equations which can be expressed as gap equation. The pairing depends only on one parameter, namely the effective scattering length in the Hamiltonian  $a = -0.41\text{fm}$  that was obtained from fitting the pairing gaps to the odd-even staggering binding energies of neutrons and protons in nuclei (see Fig. 5). The shell structure and the average pairing is well reproduced. If nuclei were to be placed in the pairing phase diagram of Fig. (4) they would lie in the transition region between the single-shell, multi-shell and single-level pairing regions. Because the multi-shell increase pairing and single-level decrease pairing the average gaps are to a good approximation given by the supergap of Eq. (19). Adjusting the h.o. frequency and oscillator length to that in nuclei with constant central densities of  $n = 0.15\text{fm}^{-3}$  the supergap becomes

$$\Delta \simeq G = \frac{|a|}{0.41\text{fm}} \frac{5.5\text{MeV}}{A^{1/3}}. \quad (20)$$

The supergap predicts a  $A^{-1/3}$  scaling in good agreement with nuclear pairing data. It differs slightly from the standard  $A^{-1/2}$  scaling in the Bethe-Weiszäcker liquid-drop formula.

The supergap is robust in the sense that it does not depend on the level spectra or other details, and thus allows us to extract the effective scattering length directly.

For very large nuclei multi-shell pairing becomes increasingly important and pairing approaches that in bulk matter. With the effective nucleon coupling constant  $a = -0.41\text{fm}$  extracted from pairing gaps in finite nuclei, we can estimate the  $^1S_0$  pairing of both neutrons and protons in nuclear matter from Eq. (17)

$$\Delta \simeq 1.1\text{MeV}. \quad (21)$$

Neutron star matter has a wide range of densities and is very asymmetric,  $Z/A \simeq 0.1$ . One can attempt to estimate of the pairing gaps as function of density from the gap

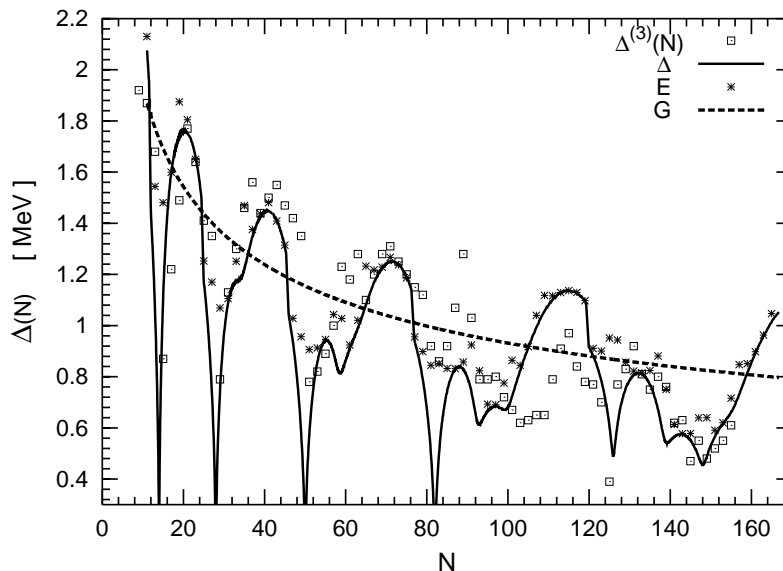


**Figure 5.** Neutron pairing  $\Delta^{(3)}(N)$  vs. the number of neutrons. The experimental values have been averaged over isotopes [37]. The calculated gaps  $\Delta$  and quasi-particle energies  $E$  are obtained from the gap equation (see text) with effective coupling strength  $a = -0.41$  fm. The supergap  $G$  is shown with dashed line. From [32].

in bulk, Eq. (17), with  $a \simeq -0.41$  fm. However, the effective interaction  $a$  is density dependent. At higher densities we expect the effective interaction to become repulsive as is the case for the nuclear mean field at a few times nuclear saturation density. At lower densities the effective scattering length should approach that in vacuum which for neutron-neutron scattering is  $a(^1S_0) \simeq -18$  fm.

Neutron stars are so cold that neutron and proton superfluidity is expected in most of the surface layers. The depinning of superfluid vortices can explain neutron star glitches in star quakes [42].

## 6. Summary and Outlook

We list the main results discussed above and add a few topics for future investigation:

- In the unitarity limit near Feshbach resonances,  $n|a|^3 \gg 1$ , where bosons and fermions interact strongly or are dense, the particle energies (and pairing gaps) scale like  $\hbar^2 n^{2/3}/m$  times an universal constant.
- For  $^{85}\text{Rb}$  bosons recent experiments [1] confirm the unitarity limit and measure a transition frequency  $\nu \simeq 5\text{kHz}$  near the Feshbach resonance in agreement with the predictions from LOCV. Experiments at other densities are underway to check the “fermion”  $n^{2/3}$  dependence of the energy per particle.
- The unitarity limit has also been confirmed for Fermi atoms near Feshbach resonances. Measurements of the universal parameter  $\beta = E_{int}/E_{kin} \simeq -0.5$  as

$a \rightarrow -\infty$  are compatible with theoretical predictions.

- The pairing gap in traps with attracting Fermi atoms is  $\Delta \simeq 0.5E_F$  near Feshbach resonances and the critical temperature  $T_c \simeq 0.5\Delta$ . Thus superfluidity may already have been achieved in recent experiments.
- Cooling further will eventually make measurements of smaller pairing gaps possible. By varying the number of particles and interaction strengths the pairing in h.o. traps with attractive Fermi atoms undergoes several pairing phases. These exhibit a wide range of pairing mechanisms that apply to many other physical systems.
- Pairing of neutrons and protons in nuclei is similar to super-pairing in atomic traps. The supergap scales as  $\Delta \simeq 5.5 \text{ MeV}/A^{1/3}$  with mass number. Nuclei also extend into the multi-level pairing regime seen as a strong shell dependence with magic numbers.
- Large nuclei approach the  $^1S_0$  pairing bulk in nuclear matter  $\Delta \simeq 1.1\text{MeV}$  for both neutrons and protons. Pairing will, however, vary with density and asymmetry in neutron star matter. Low neutron densities is also dominated by a large negative scattering length  $a(^1S_0) \simeq -18\text{fm}$  due to a Feshbach resonance in the NN channel.
- Mixing fermionic with bosonic atoms allow sympathetic cooling [5, 38, 39, 40, 41] and thus to study weaker pairing. Induced interactions between fermions and bosons generally enhance pairing [29].
- A systems of fermions with attractive interactions and two spin states will not collapse as bosanovae and supernovae, not even near a Feshbach resonance because the kinetic energy dominates,  $1 + \beta \geq 0$ . Three spin states is marginal and may be studied in  $^6\text{Li}$  where three broad Feshbach resonances lie close in magnetic field. If three or more spin states can be tuned resonantly, their attractive interaction energy should dominate as  $a \rightarrow -\infty$  and the systems collapse as “Ferminovae”.
- Optical lattices in current experiments have few atoms in each local trap and we thus expect superpairing which favors the insulator vs. conductor state.

Tabletop experiments at low temperatures at Feshbach resonances extend our studies of dilute systems to include also strongly interacting and dense Fermi and Bose systems with unitarity scaling. It will provide new insight into a new scaling region as well as BCS pairing in atomic traps. At certain interaction strengths and particle number the pairing mechanisms and superfluidity in h.o. traps with cold atoms are similar to that in nuclei and neutron star matter.

## References

- [1] N. Claussen et al., Phys. Rev. **A 67**, 060701 (2003).
- [2] K. M. O'Hara, S. L. Hemmer, M. E. Gehm, S. R. Granade, J. E. Thomas, Science **298** (2002) 2179. M. E. Gehm, S. L. Hemmer, S. R. Granade, K. M. O'Hara, J. E. Thomas, cond-mat/0212499.
- [3] T. Bourdel et al., Phys. Rev. Lett. **91**, 020402 (2003).
- [4] C. A. Regal, D. S. Jin, Phys. Rev. Lett. **90**, 230404 (2003); C. A. Regal, C. Ticknor, J. L. Bohn, D. S. Jin, cond-mat/0305028.
- [5] S. Gupta et al., Science, Vol. 300 (2003), 1723; Phys. Rev. Lett. **91**, 160401 (2003). S. Gupta, priv. comm.
- [6] M. Bartenstein et al., cond-mat/0401109.
- [7] H. Heiselberg, Phys. Rev. **A 63**, 043606 (2001); Recent Progress in Many-Body Theories (MBX 1999), cond-mat/0002056.
- [8] S. Cowell, H. Heiselberg, I.E. Mazets, J. Morales, V.R. Pandharipande, and C.J.Pethick, Phys. Rev. Lett. **88**, 210403 (2002).
- [9] V. R. Pandharipande, Nucl. Phys. A **174**, 641 (1971) and **178**, 123 (1971); V.R. Pandharipande and H.A. Bethe, Phys. Rev. C **7**, 1312 (1973); V. R. Pandharipande and K. E. Schmidt, Phys. Rev. A **15**, 2486 (1977).
- [10] E. Timmermans et al., Phys. Rev. Lett. **83**, 2691 (1999).
- [11] M. Holland, J. Park, R. Walser, Phys. Rev. Lett. **86**, 1915 (2001); M. Holland, S.J.J.M.F. Kokkelmans, M.L. Chiofalo, R. Walser, Phys. Rev. Lett. **87**, 120406 (2001).
- [12] Y. Ohashi & A. Griffin, Phys. Rev. Lett. **89**, 130402 (2002).
- [13] T. Koehler, T. Gasenzer, K. Burnett, Phys. Rev. **A 67**, 013601 (2003).
- [14] T.-L. Ho, cond-mat/0309109.
- [15] V.A. Yurovsky, A. Ben-Reuven, Phys. Rev. **A 67**, 043611 (2003).
- [16] J. Carlson, H. Heiselberg, and V. R. Pandharipande, Phys. Rev. C **63**, 017603 (2001).
- [17] H.A. Duine and H.T.C. Stoof, cond-mat/0303230, to appear in New J. Physics Focus Issue on Quantum Gases.
- [18] E. Braaten et al., Phys.Rev.Lett. **87** (2001) 160407; Phys.Rev. A **63** (2001) 063609
- [19] S. Jonsell, H. Heiselberg, C.J. Pethick, Phys. Rev. Lett. **88** (2002) 50401.
- [20] V. M. Galitskii, JETP **34**, 151 (1958).
- [21] K.A. Brueckner, C.A. Levinson, and H.M. Mahmoud, Phys. Rev. **103**, 1353 (1956); H.A. Bethe and J. Goldstone, Proc. Roy. Soc. (London), **A238**, 551 (1957).
- [22] This equation deviates slightly from the approximate expression given in Ref. [7], Eq. (14).
- [23] V. R. Pandharipande, Int. J. of Mod. Phys. **B13**, 543 (1999); G. Baym and C. J. Pethick, Ann. Rev. Astr. & Astrophysics **17**, 415 (1979). H. Heiselberg and V.R. Pandharipande, Ann. Rev. Nucl. & Part. Science **50** (2000) 481. H. Heiselberg and M. Hjorth-Jensen, Phys. Rep. **50** (2000) 481.
- [24] H. Heiselberg, C.J. Pethick, D.G. Ravenhall, Phys. Rev. Letts. **61**, 818 (1988).
- [25] J. Carlson, S-Y. Chang, V. R. Pandharipande, K. E. Schmidt, Phys. Rev. Letts. **91**, 50401 (2003).
- [26] S.J.J.M.F. Kokkelmans, G.V. Shlyapnikov, C. Salomon, cond-mat/0308384.
- [27] T-L. Ho, E. J. Mueller, cond-mat/0306187.
- [28] L. P. Gorkov & T. K. Melik-Barkhudarov, JETP **13**, 1018 (1961);
- [29] H. Heiselberg, C. J. Pethick, H. Smith and L. Viverit, Phys. Rev. Letts. **85**, 2418 (2000).
- [30] P. Nozières and S. Schmidt-Rink, J. Low Temp. Phys. **59**, 195 (1982). C. A. R. Sá de Melo, M. Randeria, and J. R. Engelbrecht, Phys. Rev. Lett. **71**, 3202 (1993).
- [31] H. T. C. Stoof, M. Houbiers, C. A. Sackett, and R. G. Hulet, Phys. Rev. Lett. **76**, 10 (1996).
- [32] H. Heiselberg, Phys. Rev. **A 68**, 053616 (2003)
- [33] H. Heiselberg and B. R. Mottelson, Phys. Rev. Lett **88**, 190401 (2002).
- [34] G. M. Bruun and H. Heiselberg, Phys. Rev. A **65**, 053407 (2002).
- [35] A. Bohr and B. R. Mottelson, *Nuclear Structure* Vols. I+II, Benjamin, New York 1969.

- [36] A. L. Fetter and J. D. Walecka, *Quantum Theory of Many-Particle Systems*, McGraw-Hill 1971.
- [37] G. Audi and A. H. Wapstra, Nucl. Phys. **A595**, 409 (1995). J. Dobaczewski et al., Phys.Rev. **C63**, 024308 (2001).
- [38] H. T. C. Stoof, Phys. Rev. **A61**, 053601 (1999).
- [39] K. E. Strecker, G. B. Partridge, R. G. Hulet, Phys. Rev. Lett. **91**, 080406 (2003)
- [40] F. Ferlaino, E. de Mirandes, G. Roati, G. Modugno, M. Inguscio, cond-mat/0312255.
- [41] J. Cubizolles, T. Bourdel, S.J.J.M.F. Kokkelmans, G. V. Shlyapnikov, C. Salomon, cond-mat/0308018.
- [42] A. Bohr, B. R. Mottelson, D. Pines, Phys. Rev. **110**, 936 (1958).